

Physicochemical and antibacterial properties of ZnO nanoparticles-modified mineral trioxide aggregate hydrated with antibiotic/chitosan solution

Propriedades físico-químicas e antibacterianas de agregado trióxido mineral modificado com nanopartículas de ZnO hidratado com solução de antibiótico/quitosana

Ismi KHUZAIMAH¹ , Sri Juari SANTOSA¹ , Fajar Inggit PAMBUDI¹ , Dyah IRNAWATI² , NURYONO¹ 

1 - Universitas Gadjah Mada, Faculty of Mathematics and Natural Sciences, Department of Chemistry. Yogyakarta, Indonesia.

2 - Universitas Gadjah Mada, Faculty of Dentistry, Department of Dental Biomaterial. Yogyakarta, Indonesia.

How to cite: Khuzaimah I, Santosa SJ, Pambudi FI, Irnawati D, Nuryono. Physicochemical and antibacterial properties of ZnO nanoparticles-modified mineral trioxide aggregate hydrated with antibiotic/chitosan solution. *Braz Dent Sci.* 2025;28(2):e4595. <https://doi.org/10.4322/bds.2025.e4595>

ABSTRACT

Mineral trioxide aggregate (MTA) modified with ZnO nanoparticles (ZnONP) and hydrated with chitosan solution denoted MTA-ZnO/Ch is a strategy to solve the MTA limitations as a pulp capping material in root canal therapy. MTA materials with high antibacterial activity and antibiotic delivery are being developed. **Objective:** This study evaluated the effect of various antibiotic additions to MTA-ZnO/Ch on mechanical and antibacterial activities. **Material and Methods:** The ZnONP, 5% (w/w), was added during preparing MTA, and the resulting gel was calcined at 1000 °C to obtain MTA-ZnO. The MTA-ZnO was hydrated with 4% chitosan in 1% acetic acid solution containing antibiotics (tetracycline, metronidazole, amoxicillin, and ampicillin) at a 1:1 ratio to produce MTA-ZnO/Ch-AB. The properties studied included compressive strength, diametral tensile strength, radiopacity, mass loss percentage, pH change, and antibacterial activity against *Pseudomonas aeruginosa* (*P. aeruginosa*) and *Enterococcus faecalis* (*E. faecalis*). **Results:** The synthesized MTA-ZnO/Ch has a compact structure, large surface area, and mesopore distribution with an average particle size of 747.04 nm. Among antibiotics investigated, only tetracycline improved the compressive and diametral tensile strengths of MTA-ZnO/Ch. Adding all investigated antibiotics did not affect the mass loss percentage (except for tetracycline reducing the mass loss), radiopacity, and the pH of the MTA-ZnO/Ch immersed saliva. Except for ampicillin addition against *E. faecalis*, which did not show antibacterial activity, antibiotics added to MTA-ZnO/Ch improved antibacterial activities against *P. aeruginosa* and *E. faecalis*. **Conclusion:** Adding tetracycline in MTA-ZnO/Ch enhanced physicochemical and antibacterial properties, and it can potentially be a conservative pulp therapy material.

KEYWORDS

Antibacterial; Antibiotics; Chitosan; Mineral trioxide aggregate; ZnO nanoparticles.

RESUMO

O agregado trióxido mineral (MTA), modificado com nanopartículas de óxido de zinco (ZnONP) e hidratado com solução de quitosana (MTA-ZnO/Qu), tem sido proposto como alternativa para superar as limitações do MTA convencional como material de capeamento pulpar em terapias endodônticas. Materiais à base de MTA com maior atividade antibacteriana e capacidade de liberação de antibióticos vêm sendo desenvolvidos. **Objetivo:** Avaliar o efeito da adição de diferentes antibióticos ao MTA-ZnO/Qu sobre suas propriedades mecânicas e atividade antibacteriana. **Material e Métodos:** As ZnONP (5% p/p) foram incorporadas ao MTA durante o preparo, e o gel obtido foi calcinado a 1000 °C para obtenção do MTA-ZnO. Este foi então hidratado com quitosana a 4% em solução de ácido acético a 1% contendo antibióticos (tetraciclina, metronidazol, amoxicilina ou ampicilina),

na proporção 1:1, resultando no composto MTA-ZnO/Qu-AB. As propriedades avaliadas incluíram resistência à compressão, resistência à tração diametral, radiopacidade, perda de massa, variação de pH e atividade antibacteriana frente a *Pseudomonas aeruginosa* (*P. aeruginosa*) e *Enterococcus faecalis* (*E. faecalis*). **Resultados:** O MTA-ZnO/Qu sintetizado apresentou estrutura compacta, ampla área superficial e distribuição mesoporosa, com tamanho médio de partícula de 747,04 nm. Dentre os antibióticos testados, apenas a tetraciclina aumentou significativamente as resistências à compressão e à tração diametral. A adição dos antibióticos não alterou a perda de massa (exceto pela tetraciclina, que reduziu esse parâmetro), radiopacidade e pH da saliva em que o material foi imerso. Todos os antibióticos melhoraram a atividade antibacteriana contra as bactérias testadas, exceto a ampicilina frente a *E. faecalis*, que não demonstrou atividade antibacteriana, os antibióticos adicionados ao MTA-ZnO/Qu melhoraram as atividades antibacterianas contra *P. aeruginosa* e *E. faecalis*. **Conclusão:** A incorporação de tetraciclina ao MTA-ZnO/Qu aprimorou suas propriedades físico-químicas e antibacterianas, destacando seu potencial como material conservador para terapias pulpares.

PALAVRAS-CHAVE

Antibacterianos; Antibióticos; Quitosana; Agregado trióxido mineral; Nanopartículas de ZnO.

INTRODUCTION

Oral and dental diseases are significant global health concerns, affecting millions of people. The community's typical dental disease is caries, which can progress to pulp disease. In conservative pulp therapy, calcium hydroxide or mineral trioxide aggregate (MTA) is needed to maintain pulp vitality in cases of conservative pulp treatment. Calcium hydroxide is cheaper and more accessible, but the results are not as optimal as when using MTA. An in-vivo study by Cervino et al. [1] showed that MTA can stimulate the proliferation of pulp cells much higher than calcium hydroxide. MTA is similar to Portland cement in that the main ingredient is fine hydrophilic particles and has the main components of tricalcium silicate, dicalcium silicate, and tricalcium aluminate, but with the addition of bismuth oxide as a radiopaque agent. This material takes 3-4 hours to harden and has a pH of 12.5 [1]. The use of MTA in health applications includes pulp capping treatment, perforation repair, root tip closure, and spurring root development in pulpotomy treatment [2].

Even though showing excellent sealing ability and biocompatibility in pulp capping applications, MTA has weaknesses, including bacterial penetration in clinical applications, which subsequently induces inflammatory responses [3]. Thus, an ideal dental material should exhibit antibacterial efficacy without detrimentally affecting its biological and physical properties. Another limitation of MTA is poor mechanical properties in the early stages of cement hydration, which causes it to wash out quickly in a liquid environment [4]. MTA must

fulfill several requirements as a capping agent, namely having antibacterial properties, adhering to dentin and restoration materials, resisting pressure when applying restoration materials, and looking radiopaque on radiographs after application [5]. In addition, pulp capping materials must have good physical properties, one of which is tensile strength, representing good adhesion ability with the tooth [6]. Efforts to overcome the limitations have been reported in previous research. Our last study proved that adding 4% chitosan to MTA provides the highest intimate contact between dentin and material interface and enhanced antibacterial activities compared to commercial MTA [7]. However, chitosan addition to MTA lowers mechanical strength at the early stages of cement hydration [8]. As the main component of MTA, compounds have been widely used to repair hard tissues such as bones and teeth due to their ability to induce mineralization [9]. Furthermore, chitosan can deposit on the surface of the dentinal tubules, resulting in more adhesion between the dentin and MTA interface [7].

ZnO nanoparticles are widely used in various biomaterials to improve their mechanical and biological properties [10]. The release of zinc ions at low concentrations can increase antibacterial activity, stimulate cell proliferation in vitro, and stimulate osteoblast cells in hard tissues such as bones and teeth. On the other hand, the presence of ZnO in MTA does not significantly change its radiopaque property; hence, the composition ratio of ZnO and Bi₂O₃ can be applied to achieve the qualified radiopacity level. The promising characteristics of ZnO and chitosan have made them suitable for modifying MTA.

Combining MTA with ZnO and chitosan improves its mechanical and antibacterial properties [10].

During the past few decades, the most effective method of infection removal caused by numerous microbes, particularly aerobes and anaerobes bacteria, has been using antibiotics or other antimicrobials incorporated in some antibiotic delivery systems. Several antibiotic-releasing systems for dental drug delivery have been reported, including chitosan film for metronidazole and levofloxacin delivery [11], chitosan-pectin and chitosan-alginate polyelectrolyte complex (PEC) films for tetracycline [12], and hydroxyapatite/chitosan composite for minocycline [13]. It is necessary to develop the pulp capping material, MTA modified with ZnONP and chitosan (MTA-ZnO/Ch), to be used as an antibiotic delivery system. This research aims to evaluate the effect of adding various antibiotics on the physicochemical and antibacterial properties of MTA-ZnO/Ch. It is hypothesized that adding antibiotics increases the antibacterial activity of MTA without reducing the essential properties of MTA/ZnO/Ch for a pulp capping agent. In this research, four antibiotics (tetracycline, metronidazole, amoxicillin, and ampicillin) were chosen, and two bacteria, *Pseudomonas aeruginosa* (*P. aeruginosa*) and *Enterococcus faecalis* (*E. faecalis*), were tested.

MATERIAL AND METHODS

Materials

The materials used for preparing MTA were bismuth (III) oxide (Bi_2O_3) powder, zinc oxide nanoparticles (ZnONP) powder, 25% ammonia (NH_3) solution, tetraethyl orthosilicate (TEOS), calcium carbonate (CaCO_3) powder, and aluminum nitrate nonahydrate ($\text{Al}_2(\text{NO}_3)_3 \cdot 9\text{H}_2\text{O}$). Hydration of MTA material used chitosan ($\text{C}_6\text{H}_{11}\text{O}_4$ 99% purity Sigma Aldrich, USA) 4% solution in acetic acid (CH_3COOH 99% purity Merck, USA) 1% solution. Three antibiotic powders in pharma-grade were ampicillin, amoxicillin, and tetracycline, while metronidazole was used in an aqueous solution with a concentration of 5000 mg/L. Chemicals used to prepare the artificial saliva included potassium chloride (KCl) powder, sodium chloride (NaCl) powder, sodium bicarbonate (NaHCO_3) powder, anhydrous sodium hydrogen phosphate (Na_2HPO_4) powder, potassium dihydrogen phosphate (KH_2PO_4) powder, urea ($\text{CH}_4\text{N}_2\text{O}$) powder, potassium thiocyanate (KSCN) powder,

and 1 M hydrochloric acid (HCl) solution. OXOID ciprofloxacin test disc, bacteria of *Pseudomonas aeruginosa* (*P. aeruginosa*) (ATCC 10145) and *Enterococcus faecalis* (*E. faecalis*) (ATCC 29212), 70% ethanol solution, 0.9% sodium chloride (NaCl) infusion, and OXOID Muller Hinton Agar media were used to test the antibacterial activity of the MTA materials.

Instrumentation

The instruments needed in this research were an attenuated total reflectance-infrared spectroscopy (ATR-IR) 8201 PC Shimadzu, X-ray diffractometer (XRD) Bruker AXS D8 Advance ECO, scanning electron microscope-energy dispersive X-ray (SEM-EDX) Jeol JSM-6510LA, and Surface Area Analyser (SAA) Quantachrome Novatouch Lx4.

Preparation of MTA modified with ZnO nanoparticles

ZnONP-modified MTA (MTA-ZnO) containing CaO, SiO_2 , Al_2O_3 , Bi_2O_3 , and ZnONP of 60%, 20%, 2%, 13% and 5%, respectively, were synthesized using a sol-gel method. A mixture of 200 mL of distilled water and 200 μL of 25% ammonia solution was stirred for 10 minutes, then 6.93 mL of TEOS was added and stirred for 10 minutes. CaCO_3 powder (10.71 g) was added to the solution and allowed to stand for 30 minutes while stirring at 80 °C. The white suspension was then mixed with 0.70 g of $\text{Al}_2(\text{NO}_3)_3 \cdot 9\text{H}_2\text{O}$ and 0.50 g (5%) of ZnO and stirred for 1 hour at 80 °C. The suspension was evaporated while stirring at 120 °C for 90 minutes. Then, the gel was heated at 100 °C for 2 hours. The resulting powder was then calcinated at 1000 °C for 3 hours. The powder was pulverized, and 13% Bi_2O_3 (1.3 g) was added and sieved with a 200 mesh sieve [7].

Hydration of MTA-ZnO with chitosan and antibiotic solution

MTA-ZnO samples were hydrated using a liquid phase prepared by mixing a 4% (w/v) chitosan (Ch) in 1% acetic acid solution and a 1500 ppm antibiotic solution with a volume ratio of 1:1. Antibiotic types were tetracycline (TC), metronidazole (MET), amoxicillin (AMX), and ampicillin (AMP). The ratio of MTA material mass (g) to liquid volume (mL) was 2:1. The hydrated MTA samples denoted MTA-ZnO/Ch, MTA-ZnO/Ch-TC, MTA-ZnO/Ch-MET, MTA-ZnO/Ch-AMX,

and MTA-ZnO/Ch-AMP were then molded in acrylic cylinder molds according to ISO 9917-1 standard with 4 mm diameter (d) and 6 mm high (t) for compressive strength test; d=4 mm and t=3 mm for diametral tensile strength test, pH change, mass loss percentage and antibacterial activity test. For the radiopacity test, the sample size is d=5 mm and t=1 mm. In addition, the materials were characterized by XRD, SEM-EDX, ATR-IR, and SAA, as well.

Measurement of compressive strength and diametral tensile strength

MTA samples that had been hydrated for 24 hours were tested with a Universal Testing Machine (UTM) in triplicate (n=3) following ISO 9917 to produce a value in MPa. Each sample was tested with a pressure and force of 0.01 N, pre-load speed of 300 mm/min, and test speed of 10 mm/min. The maximum load required to break the sample was recorded as the mechanical test value for compressive strength and diametral tensile strength.

Radiopacity measurement

The radiopacity of the MTA samples was measured following ISO 6876; 9971-1 and ANSI/ADA in triplicate using ImageJ software for calculating Al distance (mm). The samples were hydrated and then printed with a size of d = 5 mm and t = 1 mm. The molded hydrated samples were left at room temperature (29 °C) for 24 hours. Next, the sample was placed next to the aluminum step wedge and irradiated with 7 mA X-rays at 70 kV. The distance between the specimen and the X-ray source was 30 cm with an exposure time of 0.2 seconds. The pellet sample was placed next to the aluminum step wedge with a standard 1-13 mm thickness. The radiopacity was determined based on the value of X-ray intensity that can penetrate the MTA pellet material and aluminum step wedge. The radiopacity was calculated by comparing the thickness of the aluminum step wedge, which was calculated using Equation 1.

$$A = -\log\left(1 - \frac{G}{255}\right) \quad (1)$$

where A is the absorption and G is the grey scale value of the digital image of the aluminum step wedge.

Measurement of pH and mass loss percentage

The mass loss of hydrated samples was determined according to the ISO 6876 standard in an artificial saliva media prepared with an Afnor method [14]. KCl powder (1.2 g), NaCl (0.7 g), NaHCO₃ (1.5 g), Na₂HPO₄ (0.26 g), KH₂PO₄ (0.2 g), urea (0.13 g), and KSCN (0.33 g) were mixed in a 1 L glass beaker containing 500 mL of distilled water. The mixture was stirred with a magnetic stirrer until homogeneous, and the pH was adjusted to 6.8 by adding 1 M HCl. The volume was adjusted to 1 L by adding distilled water, and the solution temperature was maintained at 37 °C. In the first step in measuring pH and determining the mass loss percentage, each sample was weighed for mass and recorded as the initial mass. Each sample was immersed in 2.5 mL artificial saliva solution, and the pH of the solution was measured at intervals of 1, 3, 7, and 14 days. During the same periods, the mass was weighed, and the samples were heated at 150 °C for 7 hours. The mass of the sample before and after being immersed in saliva was used to determine the percentage of mass loss.

Antibacterial activity testing

Antibacterial activity was tested for all samples of MTA-ZnO/Ch, MTA-ZnO/Ch-TC, MTA-ZnO/Ch-MET, MTA-ZnO/Ch-AMX, MTA-ZnO/Ch-AMP. This study used ciprofloxacin (CIP) as a positive control for antibacterial testing in triplicate on each sample against *P. aeruginosa* and *E. faecalis*. At first, all apparatus and glassware used were sterilized by rinsing with 70% alcohol and then kept in an autoclave for 2 hours at 121 °C. Next, Muller Hinton Agar (MHA) media was made by weighing 19 g of MHA and dissolved with distilled water until it reached a volume of 500 mL, then heated until homogeneous. The media was sterilized using an autoclave at 120 °C for 2 hours. MHA was poured into Petri dishes about 25 mL and allowed to solidify for test treatment. Suspensions of *P. aeruginosa* and *E. faecalis* test colonies were made by transferring one bacterial colony from solid MHA media into a test tube containing 5 mL of 0.9% NaCl. Then, the suspension of test bacteria was inoculated on 0.1 mL of MHA media [15].

Antibacterial activity was tested using a well-diffusion method by embedding the sample on MHA media. The test bacterial suspension was flattened with a cotton swab on MHA media, allowed to

dry, and then incubated for 24 hours at 37 °C. The clear zone formed around the wells was observed as the zone of inhibition of antibacterial activity. The inhibition zone, representing the antibacterial activity, was measured using a caliper three times at different positions, and the values were averaged.

Statistical analysis

To evaluate the significance of the difference between tested MTA-ZnO/Ch materials groups for the parameters being assessed, we used a multiple comparison method (one-way ANOVA followed by the Tukey HSD test). Each parameter was analyzed separately, including diametral tensile, compressive strength, pH change, mass loss, radiopacity, and antibacterial activity data. P values less than 0.05 were considered statistically significant. All statistical data were calculated using SPSS (IBM Statistic 25.0) software.

Grouping the MTA-ZnO samples for properties testing, including compressive strength, diametral tensile strength, radiopacity, pH change, mass loss percentage, and antibacterial activity, are presented in Table I.

RESULTS

Characteristics of MTA-ZnO and MTA-ZnO/Ch

Crystallinity

The crystal phase of ZnO-modified MTA (MTA-ZnO) and MTA-ZnO hydrated with 4% chitosan in 1% acetic acid solution (MTA-ZnO/Ch) was identified based on the XRD pattern as presented in Figure 1. It is observed that almost all d-spacing indicating the crystallinity of MTA-ZnO and MTA-ZnO/Ch are not significant differences.

Dicalcium silicate (C_2S), tricalcium silicate (C_3S), and tricalcium aluminate (C_3A) components are formed during calcination at 1000 °C from the precursors, with C_2S and C_3S of about 75%, as the most significant components in determining the MTA properties. The formation of C_2S can be seen at $2\theta = 18.04^\circ$, 41.19° , 54.29° (ICDD 00-024-0037), C_3S at $2\theta = 28.67^\circ$, 29.36° , and 32.08° (ICDD 00-014-0693), C_3A at $2\theta = 39.41^\circ$, 42.34° , and 50.84° (ICDD 00-033-0251). Calcium silicate hydrate (CSH) is observed at $2\theta = 29.36^\circ$ (ICDD 00-033-0306), Zn_2SiO_4 at $2\theta = 47.24^\circ$ (ICDD 00-024-1468), $Ca(OH)_2$ at $2\theta = 34.10^\circ$,

Table I - Grouping the tested MTA-ZnO/Ch samples

No. Group	Antibiotics added	Material Code (n=3)
1	No addition (control)	MTA-ZnO/Ch
2	Tetracycline	MTA-ZnO/Ch-TC
3	Metronidazole	MTA-ZnO/Ch-MET
4	Amoxicillin	MTA-ZnO/Ch-AMX
5	Ampicillin	MTA-ZnO/Ch-AMP

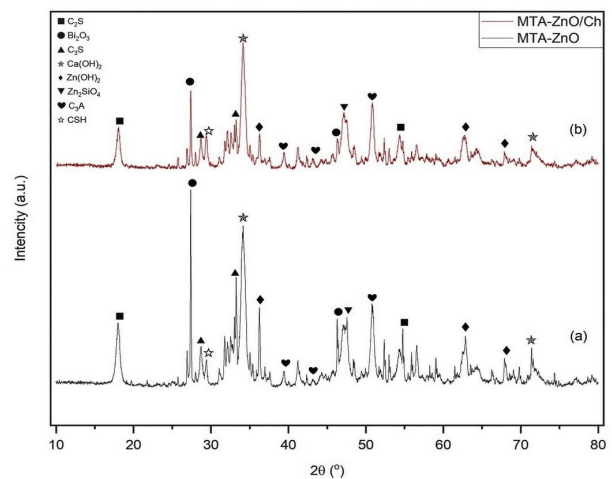


Figure 1 - XRD patterns of (a) MTA-ZnO (before hydration) and (b) MTA-ZnO hydrated with chitosan solution (MTA-ZnO/Ch).

71.55° (ICDD 00-004-0733), $Zn(OH)_2$ at $2\theta = 36.28^\circ$ and 67.92° (ICDD 00-048-1066). Bi_2O_3 peaks are detected at $2\theta = 26.89^\circ$, 27.38° , and 47.24° (ICDD 00-014-0659). The characteristic intensity of C_2S and C_3S peaks decreases in MTA-ZnO/Ch (Figure 1b), and the increase in CSH peak indicates that hydration occurs.

Morphology

The SEM image is expressed in Figure 2a, and based on the SEM image, the particle size distribution was determined with ImageJ and Origin on MTA-ZnO/Ch, resulting in an average size of 747.04 nm (Figure 2b). ZnO is indicated by the presence of fine globules scattered around the MTA. SEM images of MTA-ZnO/Ch show a dense structure with tiny pores following the porosity analysis.

Surface area, porosity, and pore size distribution

MTA-ZnO/Ch was characterized with an SAA for surface area analysis and porosity based on N_2 gas adsorption-desorption via the Brunauer-Emmett-Teller (BET) method. At the same time, pore size distribution was analyzed using the

Barrett-Joyner Halenda (BJH) method. The test results are presented in Table II.

Based on the data in Table II, modification of MTA with ZnO nanoparticles and chitosan increases the surface area and decreases the total pore volume and average pore diameter compared to MTA without modification.

Effect of antibiotics on MTA-ZnO/Ch properties

Functional groups

FTIR spectra of MTA-ZnO (before hydration), MTA-ZnO/Ch (after hydration with chitosan solution), and MTA-ZnO/Ch with antibiotic addition can be seen in Figure 3. In all FTIR spectra, the wavenumber of 505 cm^{-1} shows the Bi-O vibration of the Bi_2O_3 and the Zn-O stretching vibration [16]. The C_2S and C_3S are characterized by absorption at $1000\text{--}800\text{ cm}^{-1}$. At 994 cm^{-1} , corresponding to Si-O stretching indicates stable $\gamma\text{-C}_2\text{S}$ phases. Another calcium silicate phase (Si-O stretching) at 879 cm^{-1} , indicating the presence of $\text{Si}(\text{OSi})_3\text{O-Ca}$ (C_3S). Adsorption at $1600\text{--}1350\text{ cm}^{-1}$ corresponds to -O-H bending from $\text{Ca}(\text{OH})_2$ in un-hydrated MTA/ZnO (Figure 2a). The O-H stretching vibration of $\text{Ca}(\text{OH})_2$ was observed at $3740\text{--}3640\text{ cm}^{-1}$, and the O-H bending was observed at 1500 cm^{-1} . CSH formed during the hydration is indicated by the vibration of the O-Si-O chain at 710 cm^{-1} [10].

Figures 3c-f show the spectra of MTA-ZnO/Ch with antibiotic addition. It can be seen that the antibiotics do not give a significant difference in the FTIR spectra from MTA-ZnO/Ch. It probably overlaps with the typical absorption of -CH vibration at $1600\text{--}1396\text{ cm}^{-1}$. The broad peak is observed with the antibiotic addition, and a new weak peak (due to low concentration) appears at 2900 cm^{-1} , corresponding to the -C-H vibration from chitosan and antibiotics. Those results are similar to that of $-\text{NO}_2$ from metronidazole [17], beta-lactam ring from amoxicillin and ampicillin [18], and -CH bending vibration from tetracycline [19]. The low concentration of antibiotics leads to weak absorption bands.

Compressive strength

The effect of antibiotics on the compressive strength of MTA-ZnO/Ch is presented in Figure 4a. It can be seen that MTA-ZnO/Ch-TC has a compressive strength of $8.34 \pm 0.47\text{ MPa}$, which

is higher than that of MTA-ZnO/Ch. In contrast, the compressive strength MTA-ZnO/Ch with the addition of other antibiotics (MTA-ZnO/Ch-MET,

Table II - BET area and porosity analysis of hydrated samples

Type of Analysis	MTA	MTA-ZnO/Ch
BET surface area (m^2/g)	5.15	11.40
Total pore volume (cm^3/g)	0.17	0.03
Average pore diameter (nm)	6.43	5.17

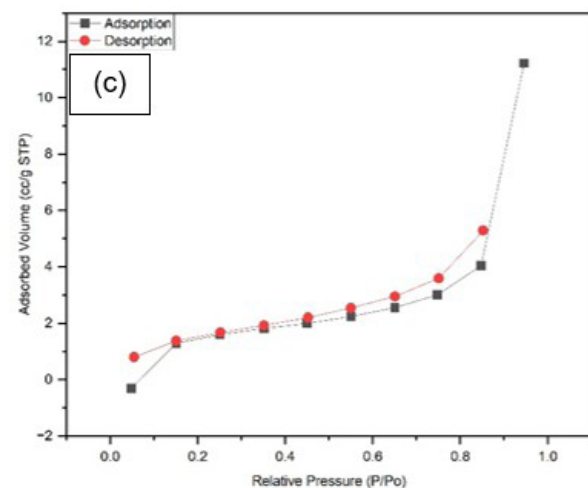
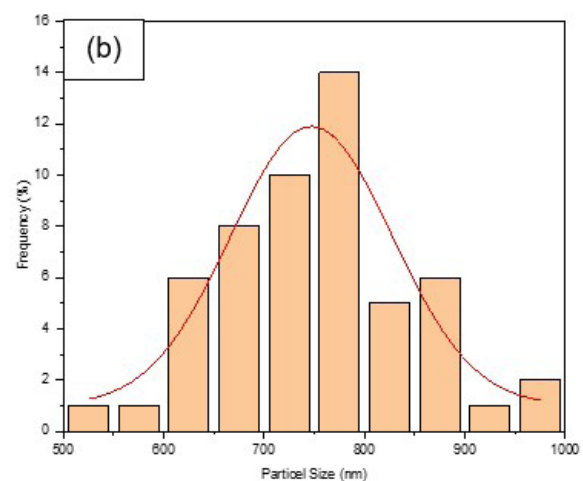
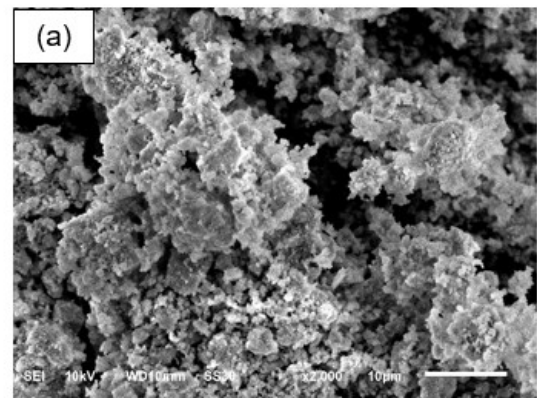


Figure 2 - (a) SEM image (2000x magnification), (b) particle size distribution histogram of MTA-ZnO/Ch, and (c) adsorption-desorption isotherm of MTA-ZnO/Ch.

MTA-ZnO/Ch-AMX, and MTA-ZnO/Ch-AMP) is smaller than MTA-ZnO/Ch (without antibiotics). The value of $p < 0.05$ was obtained through the one-way ANOVA test, meaning that the antibiotics affected the compressive strength of MTA-ZnO/Ch. However, based on the Tukey HSD test, the difference was not significant.

Diametral tensile strength

The diametral tensile strength of MTA-ZnO/Ch in the presence of antibiotics is expressed in Figure 4b. It is observed that similar to the tensile strength, MTA-ZnO/Ch-TC has the highest diametral tensile strength compared to MTA-ZnO/Ch. However, the compressive strength of MTA-ZnO/Ch-MET, MTA-ZnO/Ch-AMX, MTA-ZnO/Ch-AMP are lower than MTA-ZnO/Ch. It can be concluded that the modification of MTA with ZnO nanoparticles and chitosan and the addition of antibiotics, except tetracycline, reduce the diametral tensile strength.

Radiopacity

The calculated radiopacity is presented in Figure 4c, showing that the radiopacity of all MTA-ZnO/Ch samples, without antibiotics and with antibiotic variations, is higher than 3 mmAl. MTA-ZnO/Ch-AMX has a higher radiopacity than other samples, namely 9.63 ± 1.16 mmAl. The magnitude of this value does not indicate that the quality of radiopacity is always better than other variations of MTA. Figure 4c shows a difference in radiopacity between MTA-ZnO/Ch and MTA-

ZnO/Ch antibiotic addition. This is evidenced by the one-way ANOVA test showing $p = 0.034$, but this difference is insignificant based on the Tukey HSD test.

Mass loss percentage

Artificial saliva was chosen as the sample's immersion medium due to its characteristics being similar to those of the human biological system. The results of the mass loss test on MTA-ZnO/Ch with antibiotic addition can be seen in Figure 5a.

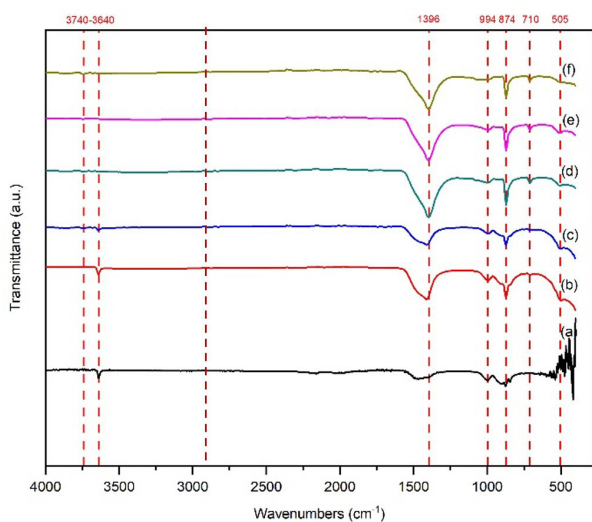


Figure 3 - IR spectra of (a) MTA-ZnO, (b) MTA-ZnO/Ch, (c) MTA-ZnO/Ch-TC, (d) MTA-ZnO/Ch-MET, (e) MTA-ZnO/Ch-AMX, (f) MTA-ZnO/Ch-AMP.

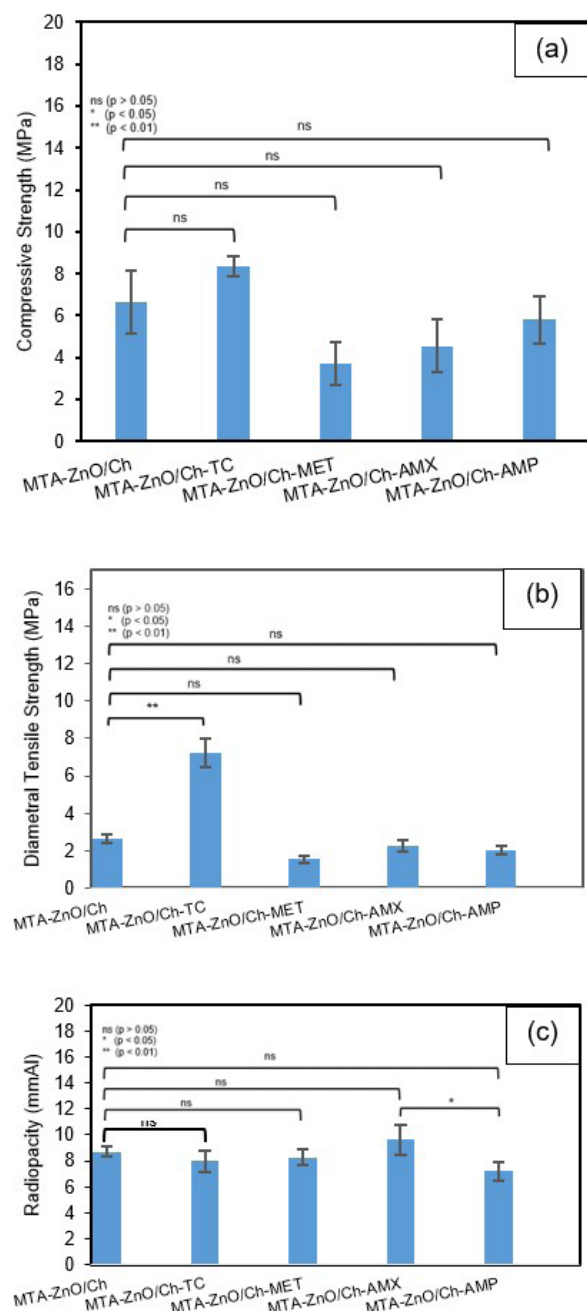


Figure 4 - (a) Compressive strength, (b) diametral tensile strength, and (c) radiopacity of MTA-ZnO/Ch variation of antibiotics.

It is evident that the mass loss percentage of each sample increases from day 1 to day 14. The antibiotics do not affect the mass loss percentage, except tetracycline, which consistently tends to be lower. However, as evidenced with the Tukey HSD test, the decrease is not significantly different.

pH testing

In the results of pH measurement (Figure 5b), the saliva immersed with MTA-ZnO/Ch-ABs has a pH of ±12.5, which is relatively constant on days 1, 3, and 7. On day 14, the pH value drops drastically to 9-10. The saliva immersed with MTA-ZnO/Ch-TC has the highest pH among the saliva immersed with other MTA materials. However, the difference is insignificant, so it can be concluded that adding antibiotics does not affect the pH of MTA-ZnO/Ch.

Antibacterial activity of MTA-ZnO/Ch with antibiotic addition

The inhibition zones, illustrating the antibacterial activity of MTA-ZnO/Ch-ABs, are presented in Figure 6.

Ciprofloxacin (10 µL) used as a positive control (the data is not included in Figure 6) was found to have an inhibition zone of 30.78 ± 1.22 mm against *P. aeruginosa* and 21.97 ± 2.07 mm against *E. faecalis*. As can be observed, MTA-ZnO/Ch used as a comparison sample showed no antibacterial property on *E. faecalis*, as indicated by the absence of an inhibition zone. However, *P. aeruginosa* shows an inhibition zone of 7.97 ± 0.49 mm, smaller than the inhibition zone of MTA-ZnO/Ch-ABs. Almost all MTA-ZnO/Ch samples with various antibiotics show inhibition zones of 8.76-11.27 mm against *P. aeruginosa* and 2.00-7.50 mm against *E. faecalis*, with higher inhibition zone than MTA-ZnO/Ch (without antibiotics). MTA-ZnO/Ch-AMX has the largest inhibition zone compared to other antibiotic variation modifications, namely 11.27 ± 0.31 mm. Figure 6 shows that adding antibiotics significantly increases the antibacterial inhibition zone (p < 0.05) of MTA-ZnO/Ch based on the one-way ANOVA test, except for ampicillin addition.

DISCUSSION

Characterization results indicated the presence of C₂S, C₃S, C₃A, Ca(OH)₂, chitosan, ZnO, and Bi₂O₃ in the synthesized MTA-ZnO/Ch. The high peaks of Bi₂O₃ indicate the natural

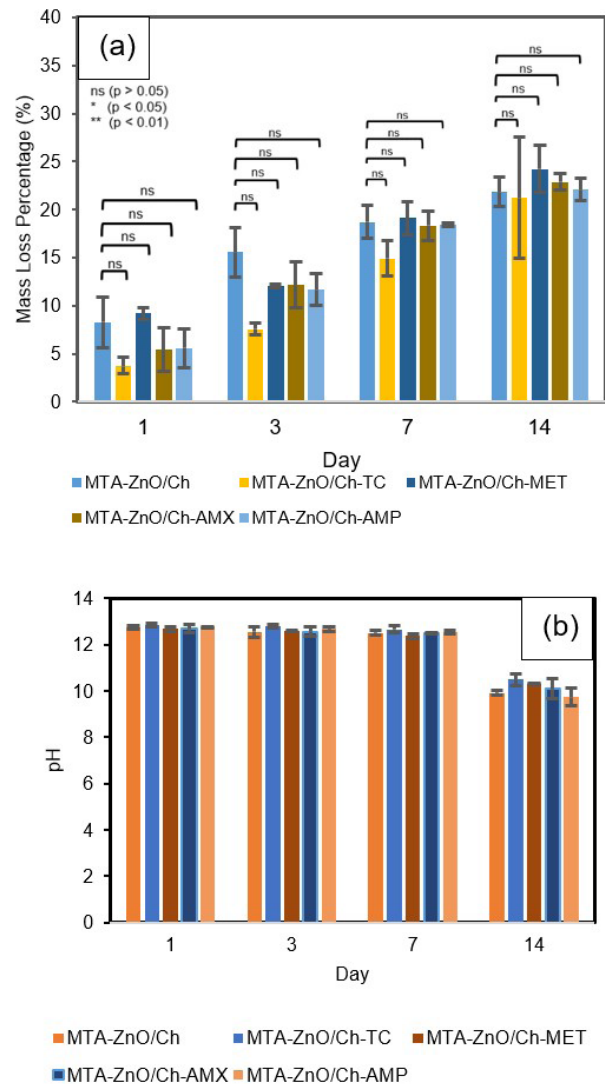


Figure 5 - (a) Mass loss percentage and (b) saliva pH after various-day immersion of MTA-ZnO/Ch-ABs.

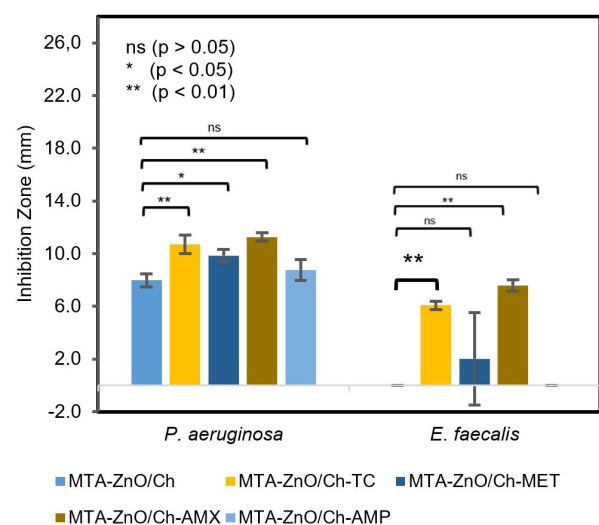


Figure 6 - Diagram of antibacterial activity presented with an inhibition zone of MTA-ZnO/Ch-AB.

crystal phase due to being added after the solid reaction [20]. C_2S and C_3S are significant components of about 75%, essential in determining the mechanical properties of hydrated MTA. In contrast, C_3A , the most reactive component, reacts quickly with water, even though it contributes less to the MTA strength [21]. Pure MTA has limitations in properties, including slow to set, creating porosity, and low antibacterial properties; hence, modification with typical components needs to be studied.

Hydration with chitosan solution does not affect the MTA phase (XRD pattern in Figure 1), except leading to decreased ZnO peak intensity. This is probably due to the formation of $Zn(OH)_2$ bonded to the CSH chain, which increases the hydration rate of C_3S [22]. Figure 2b shows that the average size of MTA-ZnO/Ch is 747.04 nm. Meanwhile, the average particle size of MTA without modification is currently 1.5-40 μm . This shows that modification with ZnONP decreases the particle size due to the formation of zinc silicate. The smaller radius of zinc ions than calcium ions gives a shorter bond length between Zn-Si compared to Ca-Si, resulting in denser cement grains and increasing the physical strength of MTA [10]. The added ZnONP partially reacts with SiO_2 by replacing Ca^{2+} to form zinc silicate (Zn_2SiO_4). This substitution can occur due to their similar ionic charges [23]. In addition, the large surface area allows good cell adhesion to interact with cells within the root canal, thereby increasing contact with dentin [24].

Based on the data in Table II, chitosan reduces porosity. It strengthens the interaction between aggregates in the composite due to hydrogen bonding between the active group -OH on the chitosan molecule and the silanol group (-Si-OH) on the silicate chain. This interaction reduces the void space and thickness zone of the adjacent CSH interlayer, thus increasing the physical strength of the MTA [7]. The chitosan in the hydrated MTA improves the physicochemical properties because chitosan acts as a reinforcing polymer to reduce porosity and strengthen the interaction between aggregates in the composite. In addition, chitosan enhances the adhesion between the cement matrix and chitosan, increasing the cement plasticity. According to Mariyam et al. [7], chitosan polymers are assumed to intercalate in the CSH interlayer and further form hydrogen bonds between the active -OH group on the chitosan molecule and the silanol

group (-Si-OH) on the CSH silicate chain. These intercalations and interactions reduce space, make the CSH interlayer closer, and increase MTA's physicochemical strength. Adding chitosan to MTA neutralizes the acidic environment through the protonation of amino groups and increases the pH of the immersion solution. Therefore, the corrosion, pore formation, and micro-leakage can be minimized as the acidity is reduced [7].

Antibiotics added to MTA-ZnO/Ch reduce mechanical properties, including compressive and shear tensile strength (Figure 4). This is following the research of Hegde and Arora [25], which states that the addition of DAP (double antibiotic paste) has a minimal effect on the compressive strength of ProRoot MTA[®] compared to the addition of TAP (triple antibiotic paste) and the compressive strength value decrease as the concentration of antibiotics added increases. Antibiotics can penetrate the root canal wall and bind with dentin and calcium ions to form insoluble complexes through chelation. Antibiotics can create an acidic environment in the root canal that can affect the binding of calcium silicate-based materials in the dentinal tubules. Unlike other antibiotics, the data shows that adding tetracycline on MTA-ZnO/Ch increases the compressive strength and diametral tensile strength. It is probably because the rich number of hydroxyl groups in tetracycline molecules interact with hydroxyl groups in chitosan to form glycoside bonds by releasing H_2O molecules, which makes the distance between chitosan chains shorter [26], leading to lower solubility of the material.

The result aligns with data in Figure 5a, indicating that the MTA-ZnO/Ch-TC sample shows a minimal mass loss percentage compared to other samples. According to the American Dental Association (ADA), the solubility used as a root canal sealer must have a value smaller than 3%. From the results of this study, only MTA-ZnO/Ch-TC is close to the allowed standard, which is 3.71% on day 1. Fridland and Rosado [27] obtained data that the solubility of MTA was 13-14% when soaked in distilled water for 14 days with a water/MTA powder ratio of 0.33%. With the same ratio, Gandolfi et al. [28] reported the solubility of MTA Plus, MTA Plus gel, and ProRoot MTA samples after soaking in distilled water for 14

days, namely 18.51%, 14.62%, and 10.79%, respectively. Therefore, due to the enhanced physicochemical properties and low mass loss percentage, adding tetracycline positively affects MTA-ZnO/Ch and its potential as pulp capping material in clinical applications.

Even though in this study, all MTA samples experienced mass loss, the solubility of components does not always have a negative effect. Fridland and Rosado [27] found that calcium hydroxide was the main compound released by MTA upon soaking. These hydroxides may be responsible for MTA's beneficial properties with dental and periapical tissues. Zbańska et al. [29] reported the regeneration of new cementum from MTA as a unique phenomenon that may be due to its sealing ability, biocompatibility, high pH, or the release of calcium hydroxide that can activate cement oblasts to lay down the matrix for cement genesis.

The radiopacity of MTA-ZnO/Ch materials, without and with antibiotic additions, is higher than 3 mmAl. This value follows the standard values of ISO 6876: 2012 and ANSI/ADA number 57. Kang et al. [30] stated that root-end filling materials should be distinguishable from bone and root adjacent to dentin for easy differentiation during treatment. In contrast, materials with radiopacity values smaller than 3 mmAl cannot be distinguished. Adding bismuth oxide to MTA increases the radiopacity without damaging physical properties. The combination of Portland cement with bismuth oxide positively correlates with radiopacity and the added bismuth oxide concentration. ZnO is a radiopaque agent commonly used in endodontic materials [31]. The radiopacity value of Bi₂O₃ is higher than ZnO due to its atomic density, but when ZnO is added to MTA, it significantly improves its physicochemical properties without losing its radiopacity. Adding chitosan with higher concentration reduces the radiopacity due to the absence of radiopacification properties in chitosan material [10]. In other words, the radiopacity of MTA-ZnO/Ch-ABs does not change and meets the pulp capping material standard.

MTA-ZnO/Ch, with the addition of antibiotics, has a pH of ± 12.5 , which is relatively constant on days 1, 3, and 7, then drops to 9-10 on day 14. Theoretically, if the pH is high, the concentration of Ca²⁺ in water is high. Ca²⁺ ions bind OH⁻ from H₂O so that OH⁻ species in water are also higher, and the pH increases [32]. Zn(OH)₂ and calcium hydroxyzincate solubility

rise in a solution with higher alkalinity, leading to an elevated pH level. Therefore, a large amount of Zn(OH)₂ and calcium hydroxyzincate species can increase the pH value in hydrated products. Even in lower Ca²⁺ concentrations, zinc ions can dissolve and form zincate ions. In addition, a high pH environment causes apatite precipitation at the material-dentin interface, resulting in excellent sealing and occlusion ability of dentinal tubules [10].

Adding antibiotics causes different effects on the antibacterial activity. The MTA-ZnO/Ch was used as a comparison sample, and MTA-ZnO/Ch-AMP showed no antibacterial activity against *E. faecalis*. Adding other antibiotics (TC, MET, and AMX) led to antibacterial activity in a 2.00-7.50 mm range. *E. faecalis* bacteria can survive in very extreme environments, including very alkaline pH and high salt concentrations [33]. Ampicillin antibiotics have a beta-lactam ring structure that binds to penicillin-binding protein (PBP) on the bacterial cell wall. This bond inhibits cell wall formation and causes damage to the bacterial cell wall structure. However, this method is less effective when used on microorganisms that have beta-lactam enzymes that work by breaking the beta-lactam ring in the penicillin group. As a result, the damaged beta-lactam ring cannot bind to PBP, so its function as an inhibitor of cell wall formation is inefficient [34]. According to Moon et al. [35], reduced ampicillin susceptibility in enterococci is due to the expression of a low-affinity class B PBP called PBP4 in *E. faecalis*. Although increased resistance in *E. faecalis* strains is less common, it may arise after prolonged beta-lactam treatment, leading to mutations in PBP4.

In contrast, MTA-ZnO/Ch had an inhibition zone of 7.97 ± 0.49 mm, lower than the inhibition zone of MTA-ZnO/Ch with various antibiotics (8.76-11.27 mm). These results agree with previously reported research. Zbańska et al. [29] reported that pure MTA found lower antibacterial properties than antibacterial material-modified MTA. Pure MTA is only effective against facultative bacteria and less effective against anaerobic bacteria. Adding ZnONP and chitosan to MTA is an alternative to improve its antibacterial properties as a pulp capping material [10]. The antibacterial mechanism of ZNONP is similar to other nanoparticles, which causes an increase in cell wall membrane permeability, release of cytoplasmic content, and cell death [36].

In comparison, the antibacterial mechanism of chitosan is caused by its ability to bind to negatively charged bacterial cell membranes, resulting in increased permeability and, ultimately, cytoplasmic leakage and bacterial cell death [37].

MTA-ZnO/Ch-TC and MTA-ZnO/Ch-AMX had higher inhibition zones than MTA-ZnO/Ch (without antibiotics) for both tested bacteria. By combining the mechanical properties, in which adding tetracycline increases the compressive strength and diametral tensile strength, it can be concluded that MTA combined with ZnO, chitosan, and tetracycline is a potential biomaterial applied for pulp capping treatment. This research is a primary step to finding applicable clinical biomaterial; further investigation is still necessary, including biocompatibility, antibiotic release kinetics, antibacterial activity against anaerobic bacteria, and in-vivo tests.

CONCLUSIONS

ZnO nanoparticle-modified mineral trioxide aggregate (MTA-ZnO) hydrated using a solution of chitosan in 4%(w/v) acetic acid solvent indicated the formation of CSH, C₂S, C₃S, C₃A, ZnSiO₄, and Bi₂O₃ components, a white solid with a diameter of 747.04 nm. Among antibiotics investigated, only adding tetracycline (MTA-ZnO/Ch-TC) reduced the mass loss and increased mechanical properties (compressive strength and diametral tensile strength). Other antibiotics tended to reduce the mechanical properties and increase the loss mass, although statistically, the reduction was insignificant. Adding antibiotics did not affect the radiopacity and pH of the solution. Meanwhile, the addition of antibiotics increased the antibacterial activity against both *P. aeruginosa* and *E. faecalis*, except for the MTA-ZnO/Ch-AMP against *E. faecalis*, which showed no antibacterial activity. MTA modified with ZnONP/Ch-TC shows potential material for pulp capping treatment incorporated with antibiotic delivery. Further investigation is ongoing by testing the slow-release kinetics of antibiotics, biocompatibility, and in-vivo experiments.

Acknowledgements

The authors thank the Directorate of Research, Technology, and Community Service, Directorate

General of Higher Education, Research, and Technology, Ministry of Education, Culture, Research, and Technology, Republic of Indonesia through the Regular Fundamental Research (PFR) Scheme with the contract number: 2660/UN1/DITLIT/PT.01.03/2024 for the financial support.

Data availability

All the data are included in the manuscript.

Author's Contributions

IK, DI: Writing – Original Draft Preparation, Methodology, Formal Analysis, Data Curation. SJS, FIP: Writing – Review & Editing, Data Curation. N: Conceptualization, Writing – Review & Editing, Supervision, Methodology, Funding Acquisition.

Conflict of Interest

No conflicts of interest declared concerning the publication of this article.

Funding

The authors thank the Directorate of Research, Technology, and Community Service, Directorate General of Higher Education, Research, and Technology, Ministry of Education, Culture, Research, and Technology, Republic of Indonesia for the financial support through the Regular Fundamental Research (PFR) Scheme with the contract number: 2660/UN1/DITLIT/PT.01.03/2024.

Regulatory Statement

This study followed all the provisions of the Ethical Commission of the Faculty of Dentistry, Universitas Gadjah Mada, under letter number 8/UN1/KEP/ FKG-RSGM/EC/2024.

Disclosure

The research study was performed as part of Universitas Gadjah Mada.

REFERENCES

1. Cervino G, Laino L, D'Amico C, Russo D, Nucci L, Amoroso G, et al. Mineral trioxide aggregate applications in endodontics:

- a review. *Eur J Dent.* 2020;14(4):683-91. <http://doi.org/10.1055/s-0040-1713073>. PMID:32726858.
2. Gürcan AT, Şişmanoğlu S, Sengez G. Effect of different adhesive strategies on the microshear bond strength of calcium-silicate-based materials. *J Adv Oral Res.* 2022;13(2):191-9. <http://doi.org/10.1177/23202068221118979>.
 3. Tsesis I, Elbahary S, Venezia NB, Rosen E. Bacterial colonization in the apical part of extracted human teeth following root-end resection and filling: a confocal laser scanning microscopy study. *Clin Oral Investig.* 2018;22(1):267-74. <http://doi.org/10.1007/s00784-017-2107-1>. PMID:28349219.
 4. Kim H-J, Lee D, Cho S, Jang J-H, Kim SG, Kim S-Y. Improvement of the bonding properties of mineral trioxide aggregate by elastin-like polypeptide supplementation. *Scanning.* 2019;2019:3484396. <http://doi.org/10.1155/2019/3484396>. PMID:31531154.
 5. Pushpalatha C, Dhareshwar V, Sowmya SV, Augustine D, Vinothkumar TS, Renugakshmi A, et al. Modified mineral trioxide aggregate - a versatile dental material: an insight on applications and newer advancements. *Front Bioeng Biotechnol.* 2022;10:941826. <http://doi.org/10.3389/fbioe.2022.941826>. PMID:36017346.
 6. Jang Y, Song M, Yoo IS, Song Y, Roh BD, Kim E. A randomized controlled study of the use of proroot mineral trioxide aggregate and endocem as direct pulp capping materials: 3-month versus 1-year outcomes. *J Endod.* 2015;41(8):1201-6. <http://doi.org/10.1016/j.joen.2015.03.015>. PMID:25933707.
 7. Mariyam M, Sunarintyas S, Nuryono N. Improving mechanical, biological, and adhesive properties of synthesized mineral trioxide aggregate by adding chitosan. *Inorg Chem Commun.* 2023;149:110446. <http://doi.org/10.1016/j.inoche.2023.110446>.
 8. Subhi H, Husein A, Mohamad D, Nurul AA. Physicochemical, mechanical and cytotoxicity evaluation of chitosan-based accelerated portland cement. *J Mater Res Technol.* 2020;9(5):11574-86. <http://doi.org/10.1016/j.jmrt.2020.07.108>.
 9. Hu D, Ren Q, Li Z, Zhang L. Chitosan-based biomimetically mineralized composite materials in human hard tissue Repair. *Molecules.* 2020;25(20):4785. <http://doi.org/10.3390/molecules25204785>. PMID:33086470.
 10. Mariyam M, Sunarintyas S, Yuliatun L, Irmawati D, Hatmanto AD, Nuryono N. Physicochemical and antibacterial properties of ZnO/chitosan-modified mineral trioxide aggregate composites. *Case Stud Chem Environ Eng.* 2024;9:100749. <http://doi.org/10.1016/j.csee.2024.100749>.
 11. Khan G, Yadav SK, Patel RR, Nath G, Bansal M, Mishra B. Development and evaluation of biodegradable chitosan films of metronidazole and levofloxacin for the management of periodontitis. *AAPS PharmSciTech.* 2016;17(6):1312-25. <http://doi.org/10.1208/s12249-015-0466-y>. PMID:26689408.
 12. Kassem AA, Ismail FA, Naggar VF, Aboulmagd E. Preparation and evaluation of periodontal films based on polyelectrolyte complex formation. *Pharm Dev Technol.* 2015;20(3):297-305. <http://doi.org/10.3109/10837450.2013.862262>. PMID:24438021.
 13. Gao H, Ge K, Xu Y, Wang Y, Lu M, Wei Y, et al. Controlled release of minocycline in hydroxyapatite/chitosan composite for periodontal bone defect repair. *Dent Mater J.* 2022;41(3):346-52. <http://doi.org/10.4012/dmj.2021-217>. PMID:35321974.
 14. Sandra Devi L, Prijatmoko D, Joelijanto R, Prasetyarini S, Herniyati, Soesetijo FXA, et al. The potential of avocado seed extract (*Persea americana*) in inhibiting the release of metal ions in cuniti and stainless steel based orthodont wire. *Int J Heal Pharm.* 2024;4(2):405-14. <http://doi.org/10.51601/ijhp.v4i2.322>.
 15. Uwzeyimana JD, Kim D, Lee H, Byun J-H, Yong D. Determination of colistin resistance by simple disk diffusion test using modified Mueller-Hinton agar. *Ann Lab Med.* 2020;40(4):306-11. <http://doi.org/10.3343/alm.2020.40.4.306>. PMID:32067429.
 16. Indurkar AR, Sangoi VD, Patil PB, Nimbalkar MS. Rapid synthesis of Bi₂O₃ nano-needles via 'green route' and evaluation of its anti-fungal activity. *IET Nanobiotechnol.* 2018;12(4):496-9. <http://doi.org/10.1049/iet-nbt.2017.0070>. PMID:29768236.
 17. Al-Khodir FAI, Refat MS. Investigation of coordination ability of Mn(II), Fe(III), Co(II), Ni(II), and Cu(II) with metronidazole, the antiprotozoal drug, in alkaline media: synthesis and spectroscopic studies. *Russ J Gen Chem.* 2017;87(4):873-9. <http://doi.org/10.1134/S107036321704034X>.
 18. Wojnárovits L, Tóth T, Takács E. Critical evaluation of rate coefficients for hydroxyl radical reactions with antibiotics: a review. *Crit Rev Environ Sci Technol.* 2018;48(6):575-613. <http://doi.org/10.1080/10643389.2018.1463066>.
 19. Meretoudi A, Banti CN, Siafarika P, Kalampounias AG, Hadjikakou SK. Tetracycline water soluble formulations with enhanced antimicrobial activity. *Antibiotics.* 2020;9(12):845. <http://doi.org/10.3390/antibiotics9120845>. PMID:33256054.
 20. Li Q, Coleman NJ. Impact of Bi₂O₃ and ZrO₂ radiopacifiers on the early hydration and C-S-H gel structure of white Portland cement. *J Funct Biomater.* 2019;10(4):46. <http://doi.org/10.3390/jfb10040046>. PMID:31635346.
 21. Kong H, Kwon KB, Park SJ, Noh WS, Lee SJ. Synthesis of C₃S, C₂S, C₃A powders using ultra-fine calcium oxide powder synthesized from Eggshell and effect of C₃A content on hardened mixed aggregates. *J Korean Powder Metall Inst.* 2019;26(6):493-501. <http://doi.org/10.4150/KPMI.2019.26.6.493>.
 22. Morales-Melgares A, Casar Z, Moutzouri P, Venkatesh A, Cordova M, Kunhi Mohamed A, et al. Atomic-level structure of zinc-modified cementitious calcium silicate hydrate. *J Am Chem Soc.* 2022;144(50):22915-24. <http://doi.org/10.1021/jacs.2c06749>. PMID:36508687.
 23. Eltohamy M, Kundu B, Moon J, Lee H-Y, Kim H-W. Antibacterial zinc-doped calcium silicate cements: bone filler. *Ceram Int.* 2018;44(11):13031. <http://doi.org/10.1016/j.ceramint.2018.04.122>.
 24. Chang SW. Chemical composition and porosity characteristics of various calcium silicate-based endodontic cements. *Bioinorg Chem Appl.* 2018;2018:2784632. <http://doi.org/10.1155/2018/2784632>. PMID:29487618.
 25. Hegde V, Arora S. Effect of intracanal medicaments on push-out bond strength of smart-seal system. *J Conserv Dent.* 2015;18(5):414-8. <http://doi.org/10.4103/0972-0707.164059>. PMID:26430308.
 26. Bayer IS. Controlled drug release from nanoengineered polysaccharides. *Pharmaceutics.* 2023;15(5):1364. <http://doi.org/10.3390/pharmaceutics15051364>. PMID:37242606.
 27. Fridland M, Rosado R. Mineral Trioxide Aggregate (MTA) solubility and porosity with different water-to-powder ratios. *J Endod.* 2003;29(12):814-7. <http://doi.org/10.1097/00004770-200312000-00007>. PMID:14686812.
 28. Gandolfi MG, Siboni F, Primus CM, Prati C. Ion release, porosity, solubility, and bioactivity of MTA plus tricalcium silicate. *J Endod.* 2014;40(10):1632. <http://doi.org/10.1016/j.joen.2014.03.025>. PMID:25260736.
 29. Zbańska J, Herman K, Kuroпка P, Dobrzyński M. Regenerative endodontics as the future treatment of immature permanent teeth. *Appl Sci.* 2021;11(13):6211. <http://doi.org/10.3390/app11136211>.
 30. Kang TY, Choi JW, Seo KJ, Kim KM, Kwon JS. Four different commercial root-end filling materials: a comparative study. *Materials.* 2021;14(7):1693. <http://doi.org/10.3390/ma14071693>.

31. Khan S, Fareed M, Kaleem M, Uddin S, Iqbal K. An updated review of mineral trioxide aggregate part-1 : compositional analysis, setting reaction and physical properties. *J Pak Dent Assoc.* 2014;23(4):140-7.
32. Ashraf W, Olek J. Carbonation behavior of hydraulic and non-hydraulic calcium silicates: potential of utilizing low-lime calcium silicates in cement-based materials. *J Mater Sci.* 2016;51(13):6173-91. <http://doi.org/10.1007/s10853-016-9909-4>.
33. Evans M, Davies JK, Sundqvist G, Figdor D. Mechanisms involved in the resistance of *Enterococcus faecalis* to calcium hydroxide. *Int Endod J.* 2002;35(3):221-8. <http://doi.org/10.1046/j.1365-2591.2002.00504.x>. PMID:11985673.
34. Rice LB, Desbonnet C, Tait-Kamradt A, Garcia-Solache M, Lonks J, Moon TM, et al. Structural and regulatory changes in PBP4 trigger decreased β -lactam susceptibility in *Enterococcus faecalis*. *Am Soc Microbiol.* 2018;9(2):e00361-18. <http://doi.org/10.1128/mBio.00361-18>.
35. Moon TM, D'Andréa ÉD, Lee CW, Soares A, Jakoncic J, Desbonnet C, et al. The structures of penicillin-binding protein 4 (PBP4) and PBP5 from *Enterococci* provide structural insights into β -lactam resistance. *J Biol Chem.* 2018;293(48):18574-84. <http://doi.org/10.1074/jbc.RA118.006052>. PMID:30355734.
36. Ibrahim AIO, Moodley DS, Petrik L, Patel N. Use of antibacterial nanoparticles in endodontics. *SADJ.* 2017;72(3):105-12.
37. Li J, Zhuang S. Antibacterial activity of chitosan and its derivatives and their interaction mechanism with bacteria: current state and perspectives. *Eur Polym J.* 2020;138:109984. <http://doi.org/10.1016/j.eurpolymj.2020.109984>.

Nuryono**(Corresponding address)**

Universitas Gadjah Mada, Faculty of Mathematics and Natural Sciences,
Department of Chemistry, Yogyakarta, Indonesia.
Email: nuryono_mipa@ugm.ac.id

Date submitted: 2024 Nov 24
Accept submission: 2025 May 02